Intersubband absorption in quantum wire with a convex bottom in a magnetic field

2006 J. Phys.: Condens. Matter 18 S2161

(http://iopscience.iop.org/0953-8984/18/33/S31)

INSTITUTE OF PHYSICS PUBLISHING JOURNAL OF PHYSICS: CONDENSED MATTER

J. Phys.: Condens. Matter **18** (2006) S2161–S2167 doi:10.1088/0953-8984/18/33/S31

Intersubband absorption in quantum wire with a convex bottom in a magnetic field

M G Barseghyan, A Kh Manaselyan and A A Kirakosyan

Department of Solid State Physics, Yerevan State University, Alex Manookian 1, Yerevan 375025, Armenia

E-mail: amanasel@server.physdep.r.am

Received 10 January 2006
Published 4 August 2006
Online at stacks.iop.org/JPhysCM/18/S2161

Abstract

The electron states in a cylindrical quantum well with a convex bottom in a magnetic field directed along the wire axis are investigated. The electron wavefunctions, depending on the quantum well characteristics and the magnetic field induction, are found. The absorption coefficient of a monochromatic linearly polarized light wave caused by intersubband transitions of electrons in the quantum wire is calculated. The selection rules are considered and analytical expressions for the absorption coefficient are presented for two cases of light wave polarization.

1. Introduction

The advances of modern semiconductor technologies led to the creation of low dimensional heterostructures where electrons are localized at size quantization levels [1]. These quantum wells (QW), quantum wires (QWW) and quantum dots (QD) are widely used in microelectronic and nanoelectronic devices, as well as in optoelectronics. In particular, lasers and detectors working in visual, short range and middle IR regions [2] are often based on such structures.

Among various methods of investigation of low dimensional structures the analysis of the optical absorption spectrum plays an important role. The investigation of interband light absorption in QWW has shown that it can be controlled by means of changing the sizes and shapes of the QWW, and with the help of external electric and magnetic fields [3–7].

The investigation of intraband absorption in QWW [8, 9] is very important as well. Today, the effects related to transitions of charge carriers from the localized levels to continuum states are intensively investigated, because of their use in new type IR receivers [10, 11].

In the present work the electronic states are investigated and the intersubband absorption coefficient of a monochromatic light wave is calculated for the semiconductor cylindrical QWW with a convex bottom in a magnetic field, directed along the wire axis. The

selection rules are revealed and analytical expressions for the absorption coefficient are found, depending on the wire parameters, magnetic field induction and light wave polarization.

2. Electron states

Let us consider a cylindrical QW with a convex bottom in a magnetic field. The exact profile of a QWW bottom is provided by growth conditions. So, convexity of the bottom of a $Ga_{1-x}Al_xAs/Ga_{1-y}Al_yAs$ QWW can be achieved by smoothly varying the alloy concentration y between the peak value at the QWW centre and the zero value on its border [12, 13]. To simplify the calculations we neglect the mismatch of electron effective mass in QWW and the surrounding medium. The dielectric inhomogeneity of the system is neglected as well.

The Hamiltonian of an electron in the system considered has the form

$$\hat{H} = \frac{1}{2m}\left(\hat{\vec{p}} + e\vec{A}_0\right)^2 + V(\rho), \tag{1}$$

where m is the electron effective mass, $\vec{A}_0$ is the vector potential of a magnetic field. Within the framework of the model considered the confining potential

$$V(\rho) = U_0\left(1 - \frac{\rho^2}{R^2}\right), \qquad \text{for } \rho \leqslant R; \qquad V(\rho) = V_0, \qquad \text{for } \rho > R, \tag{2}$$

where R is radius of the wire, U_0 is the convexity parameter of the QW bottom, V_0 is the height of the well wall (furthermore it is supposed that $V_0 > U_0$). For the homogeneous magnetic field, directed along the wire axis (z axis), we shall take the vector potential as $\vec{A}_0 = \vec{B} \times \vec{\rho}/2$; hence, in cylindrical coordinates only the component $A_\varphi = B\rho/2$ will be distinct from zero.

The eigenfunctions of the Schrödinger equation can be presented as

$$\psi_{nlk}(\rho, \varphi, z) = \frac{1}{\sqrt{2\pi L}} e^{i(l\varphi + kz)} g_{nl}(\rho), \tag{3}$$

where L is the length of the wire, k is the wavenumber, n, l are quantum numbers, $g_{nl}(\rho)$ is the radial wavefunction. Using dimensionless parameters $x = \rho/a_B$, $a = R/a_B$, $\varepsilon_{nl} = E_{nl}/E_R$, $v_0 = V_0/E_R$, $u_0 = U_0/E_R$, $\gamma = a_B^2/l_B^2$, where $l_B = (\hbar/eB)^{1/2}$ is the magnetic length, $a_B = \hbar^2\chi/me^2$ is the effective Bohr radius and $E_R = me^4/2\hbar^2\chi^2$ is the effective Rydberg energy, the Schrödinger equation for a radial wavefunction is rewritten as

$$\frac{d^2g}{dx^2} + \frac{1}{x}\frac{dg}{dx} - \left(\frac{l^2}{x^2} + \frac{\gamma^2x^2}{4} + \gamma l\right) g + (\varepsilon_{nl} - v(x))\, g = 0. \tag{4}$$

The solutions of equation (4) can be presented in the form

$$g_{nl}(x) = C_1 \begin{cases} e^{-\beta x^2/2}\left(\beta x^2\right)^{|l|/2} F\left(-\nu_1, |l|+1; \beta x^2\right), & x \leqslant a, \\ C_2 e^{-\gamma x^2/4}\left(\gamma x^2/2\right)^{|l|/2} U\left(\nu_2, |l|+1; \gamma x^2/2\right), & x > a, \end{cases} \tag{5}$$

where $F(p, q; x)$ and $U(p, q; x)$ are confluent hypergeometric functions [14],

$$\beta = \frac{\left(\gamma^2a^2 - 4u_0\right)^{1/2}}{2a}, \quad \nu_1 = \frac{\varepsilon_{nl} - u_0 - \gamma l}{4\beta} - \frac{|l|+1}{2}, \quad \nu_2 = \frac{v_0 - \varepsilon_{nl}}{2\gamma} + \frac{|l|+l+1}{2}. \tag{6}$$

The normalization constants C_1 and C_2 from equation (5) are given by the expressions

$$C_1 = \left\{\int_0^a e^{-\beta x^2}\left(\beta x^2\right)^{|l|} F^2\left(-\nu_1, |l|+1; \beta x^2\right) x\, dx + C_2^2 \int_a^\infty e^{-\gamma x^2/2}\left(\gamma x^2/2\right)^{|l|} U^2\left(\nu_2, |l|+1; \gamma x^2/2\right) x\, dx\right\}^{-1/2}, \tag{7}$$

$$C_2 = \exp\left[-\left(\frac{\beta}{2} - \frac{\gamma}{2}\right)a^2\right]\left(\frac{2\beta}{\gamma}\right)^{|l|/2} \frac{F\left(-\nu_1, |l|+1; \beta a^2\right)}{U\left(\nu_2, |l|+1; \gamma a^2/2\right)}. \tag{8}$$

The eigenvalues ε_{nl} are determined from the continuity condition for the logarithmic derivative of wavefunction at $x = a$ and are roots of the equation

$$\frac{\mathrm{d}}{\mathrm{d}x}\ln\left[\mathrm{e}^{-\beta x^2/2}\left(\beta x^2\right)^{|l|/2} F\left(-\nu_1, |l|+1; \beta x^2\right)\right]_{x=a} = \frac{\mathrm{d}}{\mathrm{d}x}\ln\left[C_2\mathrm{e}^{-\gamma x^2/4}\left(\gamma x^2/2\right) U\left(\nu_2, |l|+1; \gamma x^2/2\right)\right]_{x=a}. \tag{9}$$

3. Light absorption in QWW with a convex bottom

To calculate the absorption coefficient of linearly polarized monochromatic radiation in QWW we use the known expression [15]

$$\alpha(\omega) = \frac{\chi^{1/2}}{c}\frac{2\pi}{\hbar}\sum_{i,f}\left|\langle f|\,\hat{H}'\,|i\rangle\right|^2 (f_i - f_f)\delta(E_f - E_i - \hbar\omega), \tag{10}$$

where ω and c are the frequency and velocity of the light wave, χ is the dielectric constant of the system, $\langle f|\,\hat{H}'\,|i\rangle$ is the matrix element of the electron–photon interaction, f_i, f_f are the Fermi–Dirac distribution functions for initial and final states, respectively, E_i, E_f are the energies of these states. The Hamiltonian of the electron–photon interaction is

$$\hat{H}' = -\frac{\mathrm{i}e\hbar}{mc}\left(\vec{A}\nabla\right), \tag{11}$$

where $\vec{A}$ is the vector potential of the light wave. The matrix element included in equation (10) can be presented as

$$\langle f|\,\hat{H}'\,|i\rangle = -\mathrm{i}\left(\frac{8\pi e^2\hbar^3}{m^2\chi\omega LS}\right)^{1/2} I_{fi}, \tag{12}$$

where S is the cross section of the area where the photon absorption takes place, and

$$I_{fi} = \int \psi_f^*(\vec{r})\mathrm{e}^{\mathrm{i}\vec{q}\vec{r}}\left(\vec{\xi}\nabla\right)\psi_i(\vec{r})\mathrm{d}\vec{r}. \tag{13}$$

In equation (13) $\psi_i(\vec{r})$, $\psi_f(\vec{r})$ are the wavefunctions of initial and final states, $\vec{q}$ and $\vec{\xi}$ are the wavevector and the polarization vector of the electromagnetic wave, respectively. If we write down the operator ∇ from equation (13) in cylindrical coordinates, it is possible to present I_{fi} as

$$I_{fi} = \left(\vec{e}_\rho\vec{\xi}\right) I_{fi}^{(1)} + \left(\vec{e}_\varphi\vec{\xi}\right) I_{fi}^{(2)} + \left(\vec{e}_z\vec{\xi}\right) I_{fi}^{(3)}, \tag{14}$$

where $\vec{e}_\rho$, $\vec{e}_\varphi$, $\vec{e}_z$ are the unit directing vectors, and

$$I_{fi}^{(1)} = \delta_{l,l'}\delta_{k,k'+q_z}\int_0^\infty \mathrm{e}^{\mathrm{i}q_\rho\rho} g_{n'l'}(\rho)\frac{\mathrm{d}g_{nl}(\rho)}{\mathrm{d}\rho}\rho\,\mathrm{d}\rho, \tag{15a}$$

$$I_{fi}^{(2)} = l\delta_{l,l'}\delta_{k,k'+q_z}\int_0^\infty \mathrm{e}^{\mathrm{i}q_\rho\rho} g_{n'l'}(\rho)g_{nl}(\rho)\mathrm{d}\rho, \tag{15b}$$

$$I_{fi}^{(3)} = k\delta_{l,l'}\delta_{k,k'+q_z}\int_0^\infty \mathrm{e}^{\mathrm{i}q_\rho\rho} g_{n'l'}(\rho)g_{nl}(\rho)\rho\mathrm{d}\rho. \tag{15c}$$

The quantities $I_{fi}^{(m)}$ $(m = 1, 2, 3)$ contain the selection rules for intersubband transitions and for the arbitrary direction of light wave propagation towards the axis of the wire.

We consider two special cases.

(1) The light wave propagates perpendicular to the z axes ($\vec{e}_\rho\vec{\xi} = 0, \vec{e}_\varphi\vec{\xi} = 0, \vec{e}_z\vec{\xi} = 1, q_z = 0$). With the help of equations (14) and (15*c*) for the matrix element of the electron–photon interaction (12) we obtain

$$\langle f|\,\hat{H}'\,|i\rangle = \left(\frac{8\pi e^2\hbar^3}{m^2\chi\omega LS}\right)^{1/2} k\delta_{l',l}\delta_{k',k}\int_0^\infty \mathrm{e}^{\mathrm{i}qx}g_{n'l}(x)g_{nl}(x)x\,\mathrm{d}x, \tag{16}$$

where q is the dimensionless wavevector of the photon. The presence of Kronecker symbols in equation (16) specifies selection rules $l = l'$ and $k = k'$ at intersubband transitions.

After substitution of equation (16) into equation (10) and under the assumption that final states are empty (low temperatures), for the absorption coefficient we obtain

$$\alpha(\omega) = \frac{16\pi e^2\hbar^2}{cm^2\chi^{1/2}\omega S}\sum_{nn'l}\int_0^{k_\mathrm{F}} k^2 f\left(E_{nl} + \hbar^2k^2/2m\right)\mathrm{d}k \times \left|\int_0^\infty \mathrm{e}^{\mathrm{i}qx}g_{n'l}(x)g_{nl}(x)x\,\mathrm{d}x\right|^2 \delta\left(E_{n'l} - E_{nl} - \hbar\omega\right), \tag{17}$$

where $k_\mathrm{F} = \pi n_e/2$ is the Fermi wavenumber for the one-dimensional electron gas, n_e is the linear concentration of charge carriers. It is necessary to note that for the characteristic values of $n_e \approx 10^6$ cm^{-1} CC gas can be considered strongly degenerate already at $T < 100$ K.

For the electronic transitions from the state $n = 1, l = 0$ to the states $n' = 2, l = 0$ and $n' = 3, l = 0$, for the absorption coefficient we obtain

$$\alpha(\Omega) = \frac{\alpha_0^\parallel}{\Omega}\sum_{n'=2,3}\left|\int_0^\infty \mathrm{e}^{\mathrm{i}qx}g_{n'0}(x)g_{10}(x)x\,\mathrm{d}x\right|^2 \delta\left(\varepsilon_{n'0} - \varepsilon_{10} - \Omega\right), \qquad \alpha_0^\parallel = \frac{16\pi^4e^2}{3\hbar c}\frac{n_e^3a_\mathrm{B}^4}{\chi^{1/2}S}, \tag{18}$$

where ε_{10} and $\varepsilon_{n'0}$ are the dimensionless energies of initial and final states, respectively, Ω is the dimensionless photon energy of incident light.

Let us note that for the characteristic value $\varepsilon_{20} - \varepsilon_{10} \sim 20$, the dimensionless photon wavevector $q \simeq 2 \times 10^{-2}$; hence in the wire region $qx \leqslant qa \sim 10^{-2} \ll 1$. At greater values of x due to the exponential decrease of the $g_{n0}(x)$ functions and exponent oscillations, the integrals are of the order of 10^{-3}, and $\alpha(\Omega) \sim 10^{-2}$ cm^{-1}.

(2) Now it is assumed that the light wave propagates along the z axis ($\vec{e}_\rho\vec{\xi} = 1, \vec{e}_\varphi\vec{\xi} = 0, \vec{e}_z\vec{\xi} = 0\ q_\rho = 0$). With the help of equations (14) and (15*a*) for the matrix element of the electron–photon interaction we obtain

$$\langle f|\,\hat{H}'\,|i\rangle = \left(\frac{8\pi e^2\hbar^3}{m^2a_\mathrm{B}^2\chi\omega LS}\right)^{1/2}\delta_{l,l'}\delta_{k',k+q_z}\int_0^\infty g_{n'l'}(x)\frac{\mathrm{d}g_{nl}(x)}{\mathrm{d}x}x\,\mathrm{d}x. \tag{19}$$

As long as the characteristic values are $k \sim k_\mathrm{F} \sim n_e \sim 10^6$ cm^{-1}, and $q_z \sim 10^4$ cm^{-1}, then $k' = k + q_z \approx k$ and the selection rules obtained are the same as in the previous case.

After substitution of equation (19) into equation (10), for the absorption coefficient we obtain

$$\alpha(\omega) = \frac{16\pi e^2\hbar^2}{cm^2a_\mathrm{B}^2\chi^{1/2}\omega S}\sum_{nn'l}\int_0^\infty f\left(E_{nl} + \hbar^2k^2/2m\right)\mathrm{d}k \times \left|\int_0^\infty g_{n'l'}(x)\frac{\mathrm{d}g_{nl}(x)}{\mathrm{d}x}x\,\mathrm{d}x\right|^2 \delta\left(E_{n'lk} - E_{nlk} - \hbar\omega\right). \tag{20}$$

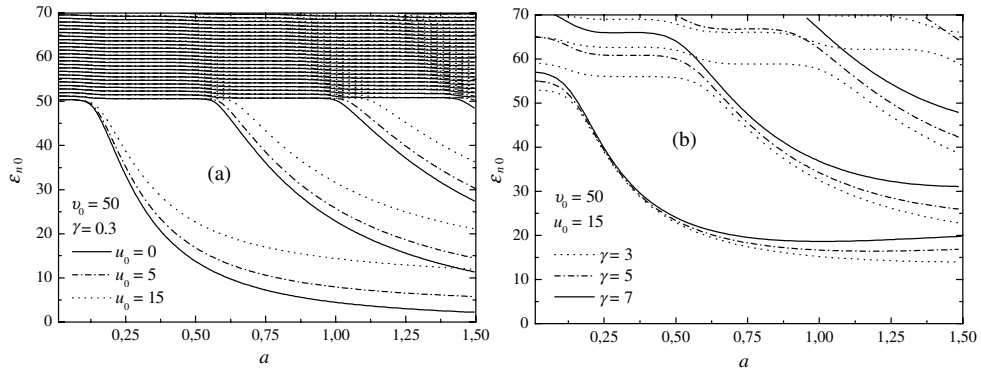

Figure 1. Dependence of the electron energy on the dimensionless radius of the QWW for various values of the convexity parameter (a) and magnetic field (b) at $l = 0$.

Taking into account the normalization condition for the distribution function and considering electronic transitions from the state $n = 1, l = 0$ to the states $n' = 2, l = 0$ and $n' = 3, l = 0$, for the absorption coefficient we obtain

$$\alpha(\Omega) = \frac{\alpha_0^{\perp}}{\Omega} \sum_{n'=2,3} \left| \int_0^{\infty} g_{n'0}(x) g'_{10}(x) x \, \mathrm{d}x \right|^2 \delta(\varepsilon_{20} - \varepsilon_{10} - \Omega), \quad \alpha_0^{\perp} = \frac{16\pi^2 e^2}{\hbar c} \frac{n_e a_{\mathrm{B}}^2}{\chi^{1/2} S}. \quad (21)$$

It is necessary to note that using this approach it is possible to take into account various sources of energy level broadening (carrier scattering, temperature spreading etc) if instead of delta functions, we insert Lorentzians in the expression for the absorption coefficient [15].

4. Discussion of the results

Numerical calculations were carried out for the GaAs/$Ga_{1-x}Al_x$As system, with parameter values $m = 0.067\, m_0$ (m_0 is the free electron mass), $\chi = 13.18$, $E_{\mathrm{R}} = 5.2$ meV, $a_{\mathrm{B}} = 104$ Å, $v_0 = 50$ (alloy concentration $x \approx 0.35$) [16]. The $\gamma = 1$ value for GaAs corresponds to the magnetic field induction value $B = 6$ T.

In figure 1(a) the dependences of the electron energy for states with $l = 0$ on the dimensionless radius of the QWW are presented for various values of u_0 at $\gamma = 0.3$. As one can see from the figure, with increase of the QWW radius, the energy levels go down and one by one enter the well because of the decrease of the role of size quantization. Note that in the area $0 \leqslant \gamma \leqslant 0.4$ the magnetic length is more than the QWW radius; therefore the magnetic field weakly influences the energy levels inside the well. Outside of the well there are discrete Landau levels. At $\gamma \to 0$ the distance between Landau levels decreases, and at $\gamma = 0$ outside the well the spectrum is continuous. In the case of $u_0 = 0$ (solid lines) the energy levels for QWW with a rectangular confining potential of finite depth are obtained. With the increase of u_0 the energy levels are shifted to the high energy region (the doted and dashed lines), which is caused by 'expulsion' of electrons from the central region of the QWW.

In figure 1(b) the dependences of the electron energy on the dimensionless radius of the QWW are presented (at $l = 0$) for various values of the magnetic field induction at the fixed value $u_0 = 15$. With increase of the QWW radius the energy levels decrease because of the decreasing role of the size quantization. With increase of γ the influence of the magnetic quantization becomes stronger, and energy levels are shifted to a high energy region (the dashed and solid lines). In figure 1(b) one can see that, as distinct from the previous case, at $\varepsilon_{n0} \geqslant v_0$

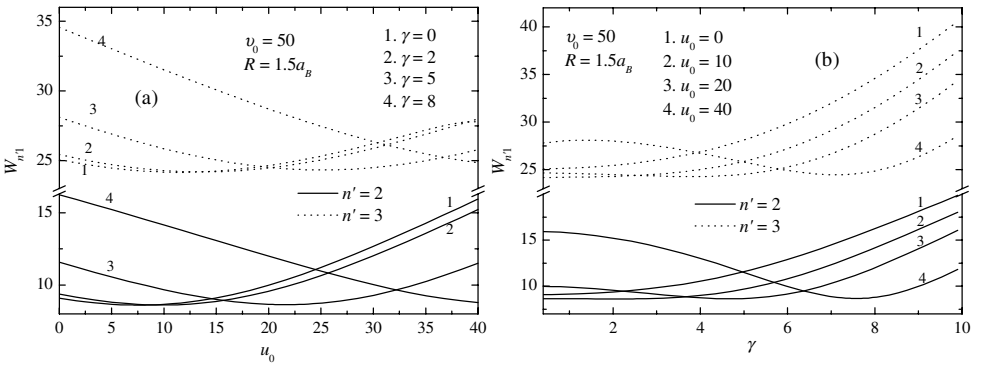

Figure 2. Dependences of the absorption threshold (a) on convexity parameter u_0 for various values of the magnetic field induction, (b) on magnetic field induction for various values of u_0.

there are discrete energy levels. Such behaviour is caused by the increase of the effective confining potential while moving away from the wire axis in the presence of a magnetic field (proportional to ρ^2).

In figure 2(a) the dependence of the light absorption threshold on the convexity parameter of the QWW bottom is presented for various values of the magnetic field induction at fixed value of the QWW radius. Solid lines correspond to transitions from the ground state to the state with $n' = 2$, and dashed lines to transitions to the state with $n' = 3$. At $\gamma = 0.3$ with the increase of u_0 the threshold value first decreases, and then starts to increase. This is caused by the fact that when u_0 is growing (still remaining small in value) the ground state energy increases faster than energies of excited states. In the case of large values of u_0 a particle in the ground state is pushed out from the central region of the QWW, and the threshold value starts to increase. With increase of the magnetic field the particle becomes located in the central region of the QWW and the region where the absorption threshold decreases becomes larger (the point of minimum is shifted to the right).

In figure 2(b) the dependence of the absorption threshold on the magnetic field induction is presented for various values of the QWW bottom convexity parameter at fixed value of the QWW radius. Solid lines correspond to the transition from the ground state to the state with $n' = 2$ and dashed lines to the state with $n' = 3$. As one can see from the figure, at small values of u_0 the absorption threshold value increases with increase of the magnetic field, because the excited states are more sensitive to magnetic field values. For large values of u_0 ($u_0 = 40$) a particle in the ground state is located near the QWW border. Therefore with increase of the magnetic field the ground state energy is promptly increased, which appears in a decrease of the absorption threshold value (there is a point of minimum).

In figure 3 the dependence of the absorption coefficient (in terms of $\alpha_0^{\perp} = 2.5 \times 10^4$ cm^{-1}) on the dimensionless photon energy for various values of u_0 (figure 3(a)) and the magnetic field induction (figure 3(b)) at a fixed value of the QWW radius $R = 1.5a_{\mathrm{B}}$ is presented for the case when the light wave propagates along the axis z. In the figures the first peak corresponds to transitions from the ground state to the state with $n' = 2$, and the second peak to ones to the state with $n' = 3$. With increase of u_0 and γ the maxima of the curves are shifted to the region of low energies because of the decrease of the absorption threshold value. It should be noted that this decrease has nonmonotonic behaviour because of the similar behaviour of the absorption threshold.

Thus introducing a new parameter, namely, the convexity of the QWW bottom, together with the magnetic field creates an additional opportunity for rather efficient control of

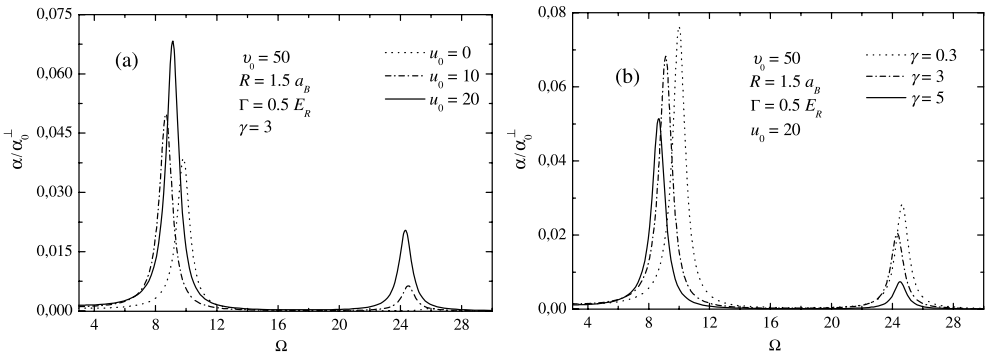

Figure 3. Dependence of the absorption coefficient on the dimensionless energy of incident light.

wavefunctions and the energy spectrum of charge carriers, which, in turn, allows one to control matrix elements, optical transition probabilities and oscillator strengths.

Acknowledgments

This work was supported by the Armenian State Programme 'Semiconductor Nanoelectronics' and by ANSEF grant No. 05-PS-nano-0811-228.

References

[1] Harrison P 1999 *Quantum Wells, Wires and Dots. Theoretical and Computational Physics* (New York: Wiley)
[2] Mao S S 2004 *Int. J. Nanotechnol.* **1** 42
[3] Aghasyan M M and Kirakosyan A A 2001 *J. Contemp. Phys. (Armenian Academy of Sciences)* **36** 20
[4] Gvozdic D M and Schlachetzki A 2003 *J. Appl. Phys.* **94** 5049
[5] Madureira J R, Degani M H and Marcelo M Z 2003 *Phys. Rev.* B **68** 161301
[6] Hashimzade F M, Ismailov T G and Mehdiyev B H 2004 *Physica* E **27** 140
[7] Lee J and Spector H N 2005 *J. Appl. Phys.* **97** 043511
[8] Galkin N G, Margulis V A and Shorokhov A V 2001 *Phys. Solid State* **43** 530
[9] Ibragimov G B 2004 *Phys. Status Solidi* b **241** 1923
[10] Ryzhii V, Khmyrova I, Ryzhii M and Mitin V 2004 *Semicond. Sci. Technol.* **19** 8
[11] Das B and Singaraju P 2005 *Infrared Phys. Technol.* **46** 209
[12] Manaselyan A Kh and Kirakosyan A A 2005 *J. Contemp. Phys. (Armenian Academy of Sciences)* **40** 223
[13] Manaselyan A Kh and Kirakosyan A A 2005 *Physica* E **28** 462
[14] Abramowitz M and Stegun I A 1970 *Handbook of Mathematical Functions with Formulas, Graphs and Mathematical Tables* (New York: Dover)
[15] Basu P K 1997 *Theory of Optical Processes in Semiconductors* (Oxford: Clarendon)
[16] Adachi S 1985 *J. Appl. Phys.* **58** R1